JB
Journals.ASM.org

Global Stress Response in a Prokaryotic Model of DJ-1-Associated Parkinsonism

Nadia Messaoudi,[a,b] Valérie Gautier,[a] Fatoum Kthiri,[a,b] Gaelle Lelandais,[f] Mouadh Mihoub,[a,b] Danièle Joseleau-Petit,[a] Teresa Caldas,[a] Chantal Bohn,[c] Leah Tolosa,[d] Govind Rao,[d] Kazuyuki Tao,[e] Ahmed Landoulsi,[b] Philippe Bouloc,[c] Gilbert Richarme[a]

Stress Molecules, Institut Jacques Monod, Université Paris, Paris, France[a]; Laboratoire de Biochimie et Biologie Moléculaire, Faculté des Sciences de Bizerte, Bizerte, Tunisia[b]; Laboratoire de Signalisation et Réseaux de Régulations Bactériens, Université Paris-Sud, CNRS UMR8621, Institut de Génétique et Microbiologie, Orsay, France[c]; Department of Chemical and Biochemical Engineering, Center for Advanced Technology, University of Maryland Baltimore County, Baltimore, Maryland, USA[d]; Radioisotope Center, University of Tokyo, Tokyo, Japan[e]; Protein Engineering and Metabolic Control, Institut Jacques Monod, UMR7592-CNRS-Université Paris, Paris, France[f]

YajL is the most closely related *Escherichia coli* homolog of Parkinsonism-associated protein DJ-1, a protein with a yet-undefined function in the oxidative-stress response. YajL protects cells against oxidative-stress-induced protein aggregation and functions as a covalent chaperone for the thiol proteome, including FeS proteins. To clarify the cellular responses to YajL deficiency, transcriptional profiling of the *yajL* mutant was performed. Compared to the parental strain, the *yajL* mutant overexpressed genes coding for chaperones, proteases, chemical chaperone transporters, superoxide dismutases, catalases, peroxidases, components of thioredoxin and glutaredoxin systems, iron transporters, ferritins and FeS cluster biogenesis enzymes, DNA repair proteins, RNA chaperones, and small regulatory RNAs. It also overexpressed the RNA polymerase stress sigma factors sigma S (multiple stresses) and sigma 32 (protein stress) and activated the OxyR and SoxRS oxidative-stress transcriptional regulators, which together trigger the global stress response. The *yajL* mutant also overexpressed genes involved in septation and adopted a shorter and rounder shape characteristic of stressed bacteria. Biochemical experiments showed that this upregulation of many stress genes resulted in increased expression of stress proteins and improved biochemical function. Thus, protein defects resulting from the *yajL* mutation trigger the onset of a robust and global stress response in a prokaryotic model of DJ-1-associated Parkinsonism.

YajL, the prokaryotic homolog of Parkinsonism-associated protein DJ-1/Park7, belongs to the PfpI/Hsp31/DJ-1 superfamily that includes chaperones (1, 2), peptidases (3, 4), and the Parkinson's disease protein DJ-1 (5, 6). The crystal structures of YajL and DJ-1 are strikingly similar (7, 8), suggesting that the proteins have similar functions. Both DJ-1 and YajL protect cells against oxidative stress (5, 9). DJ-1 has been reported to function as a weak protease (7), an oxidative-stress-activated chaperone that prevents synuclein aggregation (10, 11), a weak peroxidase that degrades hydrogen peroxide (12), a stabilizer of the antioxidant transcriptional regulator Nrf2 that allows overexpression of antioxidant enzymes (13), an apoptosis inhibitor via its interaction with Daxx (14), and a translational regulator that stimulates overexpression of selenoproteins, glutathione peroxidases, NADH dehydrogenase, and cytochrome oxidase subunits (15, 16) and uncoupling proteins (17). DJ-1 also suppresses rotenone-induced oxidative stress in dopaminergic neurons by upregulating total glutathione (GSH) and rescuing the GSH/glutathione disulfide (GSSG) ratio (18) and upregulates inducible Hsp70 (iHsp70), which results in reduced α-synuclein toxicity (19).

YajL protects bacteria against oxidative stress and oxidative-stress-induced protein aggregation, possibly through its chaperone function and control of gene expression (9). Protein aggregation depends on endogenous or exogenous oxidative stresses, since it occurs in aerobiosis but not in anaerobiosis and increases dramatically in the presence of hydrogen peroxide (9). Protein aggregates mainly contain lone subunits of multiprotein complexes, such as those of ribosomes and ATP synthase. In relation to their function in oxidative-stress protection, YajL, and DJ-1 expressed in *Escherichia coli*, function as covalent chaperones that, upon oxidative stress, form mixed disulfides with sulfenylated proteins of the thiol proteome, including chaperones, proteases, ribosomal proteins, catalases, peroxidases, and FeS proteins (20, 21); accordingly, two major FeS proteins, aconitase B and NADH dehydrogenase I, were almost inactive in the *yajL* mutant, and both YajL- and DJ-1-overproducing plasmids rescued them (21).

Gene expression profiling in Parkinson's disease brain samples led to various results highlighting genes linked to protein misfolding, the ubiquitin proteasome system, programmed cell death, mitochondrial functions, G protein signaling, and transcriptional regulation and to α-synuclein, dopamine, and synaptic genes (22). Most of the highlighted genes were downregulated, probably as a consequence of the disease, whereas others were upregulated (generally 1.2- to 2.5-fold) and may represent compensatory mechanisms in response to cell stress: overexpressed genes in the substantia nigra of the Parkinson's disease brain included genes coding for chaperones (23–25), glutathione *S*-transferases (25, 26), fibroblast and connective tissue growth factors, laminin S, STAT6, EIFG4G1, ribosomal proteins, and various unrelated proteins (23). In contradictory reports, however, several of these genes were found to be underexpressed (22, 25, 26). Thus, gene

Received 11 December 2012 **Accepted** 20 December 2012
Published ahead of print 4 January 2013
Address correspondence to Gilbert Richarme, richarme@paris7.jussieu.fr.
N.M. and V.G. contributed equally to the work.

doi:10.1128/JB.02202-12

expression profiling of the Parkinson's disease brain does not provide a clear view of whether cells set up a coherent defense against the disease or whether they merely undergo widespread damage (22).

The transcriptional profiling of the *yajL* mutant was investigated in order to understand how cells protect themselves from YajL deficiency. In contrast to the conflicting results obtained with eukaryotic cells (16), our results show that mutant cells generate a global and coherent stress response that helps alleviate the YajL defect.

MATERIALS AND METHODS

Construction of the *yajL*-disrupted strain. The chromosomal *yajL* gene of strain DY330 was replaced by a kanamycin resistance gene (*kan*) using a combination of two published protocols (27, 28) as described previously (29). Oligonucleotides 1110 (GAG TGA ATA TGA GCG CAT CTT CAC TGG TTT GCC TCG CCC CTG AAG TGT AGG CTG GAG CTT C) and 1111 (GTT TTT ACG TCG CAT CTG GTC AGA TGC GAC GTT TGC CTC ATC CGA CAC TAC ATA TGA ATA TCC TCC TTA G), used to amplify the pKD4 kanamycin resistance gene to create the Δ*yajL2*::*kan* allele, were designed to keep intact the vicinal *panE* gene after gene replacement. The Δ*yajL2*::*kan* allele was transduced to strain MG1655 by P1vir-mediated transduction (30). The kanamycin resistance cassette flanked by flippase recognition targets was removed using pCP20 (27). The resulting gene deletion was checked by PCR, and the absence of YajL was confirmed by imunoblotting (data not shown).

Preparation of bacterial extracts. Bacterial extracts were prepared by ultrasonic disruption of cells grown under aeration in LB medium to exponential phase (optical density at 600 nm [OD_{600}] = 0.3) (Branson Sonic Power Co.; 10 times for 10 s each time; 50% duty) in buffer containing 30 mM Tris, pH 8, 30 mM NaCl, 1 mM dithiothreitol, followed by centrifugation for 15 min at 30,000 × *g* at 4°C (9).

DNA microarray measurements. The *yajL* mutant and the parental strain, MG1655, were grown under aeration to exponential phase (OD_{600} = 0.3) in LB rich medium (30). Total RNAs were extracted and treated twice with DNase I (30, 31). RNA quality was monitored with a 2100 Bioanalyzer (Agilent, Santa Clara, CA). Transcriptome experiments were performed using *E. coli* Affymetrix (Santa Clara, CA) DNA chips by Cogenics (Newton, MA) according to the standard manufacturer's instructions. Hybridized arrays were stained using the Affymetrix protocol. Samples were duplicated biologically, and we calculated the average of gene expression ratios from both experiments. Genes were considered to be clearly induced if the absolute value of the expression ratio was higher than 2, and genes displaying too low a signal intensity were removed from the analysis.

Microarray analysis and data processing. After image quantification and global signal correction (following the manufacturer's instructions), the ratios between intensity values measured in the *yajL* mutant and its parent, MG1655, were calculated and normalized using the standard Lowess procedure (32). This statistical correction has the advantage of removing intensity-dependent effects in the observed $\log_2$(ratio) values and is thus well adapted to correct systematic bias related to low-intensity measures. As an additional filter, probes with low-intensity signals in the *yajL* mutant (<250) compared to background distribution were excluded from subsequent analyses. Reproducibility between results obtained with different microarray replicates was verified and used to eliminate genes with artifactual signals. Finally, to assess whether any of the cellular functions associated with the genes identified as upregulated in the *yajL* mutant (Table 1) were observed at a frequency greater than that expected by chance, *P* values were calculated as described previously (33) (hypergeometric distribution). Note that this approach was previously successfully applied (34).

GFP reporters of oxidative-stress genes. We used six oxidative-stress probes (for *soxS*, *sodA*, *zwf*, *acnA*, *katG*, and *ahpC*), composed of stress gene promoters cloned upstream of the gene coding for green fluorescent protein (GFP) (translational fusions) and inserted into pGlow-TOPO plasmids (Invitrogen) (35). Reporter plasmids were transformed into the *yajL* mutant and its parental strain; bacteria were grown in exponential phase in LB medium (30) and washed once with 63 mineral medium (30), and GFP reporter expression was quantified by measuring the GFP fluorescence of cells with a Hitachi spectrofluorimeter (excitation at 395 nm; emission at 509 nm).

Immunodetection of cellular proteins. Crude bacterial extracts (for the detection of DnaK, GroEL, and ClpB) or samples taken from cultures growing in LB medium and precipitated with 10% trichloroacetic acid (TCA) (for the detection of sigma 32 and sigma S) were separated by SDS-PAGE, transferred to nitrocellulose membranes (polyvinylidene difluoride [PVDF] membranes for sigma S), and probed with anti-DnaK (4), anti-GroEL (4), anti-ClpB (36), anti-sigma 32 (Neoclone Biotechnology), and anti-sigma S (Abcam) antibodies (37).

OxyR redox state. Bacteria were treated with trichloroacetic acid; solubilized proteins were separated by nonreducing SDS-PAGE (38), and OxyR was visualized by Western blot analysis (OxyR disulfide migrates faster than reduced OxyR). Protein bands were quantified by using ImageJ software.

H_2O_2-scavenging activities by whole cells and measure of superoxide dismutase activity. Midexponential-phase cells at an OD_{600} of 0.3 were washed with phosphate-buffered saline, resuspended in phosphate-buffered saline at an OD_{600} of 0.03, and tested for 1.5 μM H_2O_2 scavenging using the Amplex red-horseradish peroxidase assay (39). SodA and SodB activities were measured in crude bacterial extracts (prepared in 30 mM Tris, pH 7.5, 30 mM NaCl) by using an in-gel assay (40).

GSH pool and GSH/GSSG ratio. GSH and GSSG were tested in a bacterial perchloric acid extract (41) prepared from cells grown in LB medium in exponential phase and harvested at an OD_{600} of 0.3; total glutathione (GSH plus GSSG) was measured using the glutathione reductase assay. For GSSG determination, samples were pretreated for 1 h with 5% 2-vinylpyridine at 22°C before analysis by the glutathione reductase assay. Intracellular glutathione concentrations were calculated as described previously (41).

Trehalose pool. Trehalose pools were tested in bacterial perchloric acid extracts; trehalose was measured using the Megazyme trehalose assay kit (Megazyme International Ireland Limited).

Determination of mutation rates. Bacteria were grown to saturation in LB medium. The total titer and the titer of rifampin-resistant mutants were determined by plating samples on plates with no drug or 100 μg/ml rifampin; colonies were counted after 2 days of incubation.

Apurinic-site counting in DNA. DNA was purified using a DNA isolation kit, and the number of apurinic sites was assessed using the DNA damage AP Site Counting kit (Cell Biolabs Inc.) according to the manufacturer's instructions.

Microscopic observation of bacterial cells. Two milliliters of bacteria grown in LB medium to an OD_{600} of 0.1 was treated with 100 μl of 37% formaldehyde and 1.6 μl of 25% glutaraldehyde. After a 15-min incubation at 22°C, the bacteria were centrifuged, washed 3 times with M9 medium, and resuspended in 50 μl of M9 medium (30). Eight microliters of bacteria was mixed with 2 μl of the membrane-binding fluorescent dye FM4-64 (1 μg/ml) and incubated at 40°C; 8 μl of low-melting-point agarose preincubated at 40°C was added, and 3 μl of the mixture was deposited on a slide and covered with a coverslide.

Microarray data accession number. The microarray data were deposited in the Gene Expression Omnibus (GEO) (http://www.ncbi.nlm.nih.gov/geo/) under accession no. GSE42702.

RESULTS

The *yajL* mutant and the parental strain, MG1655, were grown under aeration to exponential phase (OD_{600} = 0.3) in LB rich medium (30), and their gene transcription was analyzed using oligonucleotide arrays. In addition, biochemical experiments showed that upregulation of many stress genes resulted in in-

TABLE 1 Upregulated genes in the *yajL* mutant

Gene	Gene expression ratio[a]	Product or function
Chaperones, proteases, and peptidases		
dnaK	2.1	Chaperone 70
dnaJ	2.3	Chaperone 40
grpE	2.8	Nucleotide exchange factor
clpB	1.9	Chaperone 100
tig	2.2	Chaperone, PPI
htpG	1.7	Chaperone
lon	5.1	Protease
clpX	4.4	Chaperone (proteolysis)
clpP	2.0	Protease
ftsH	5.9	Protease
pepD	3.2	Peptidase
pepP	5.1	Peptidase
pepQ	2.0	Peptidase
pepN	2.1	Peptidase
Chemical chaperones and osmotic stress		
proP	3.5	Proline transport
proVWX[b]	4.5	Glycine betaine transport
otsA	5.5	Trehalose synthesis
otsB	4.4	Trehalose synthesis
acrA	3.2	Efflux pump
acrB	2.5	Efflux pump
tolC	2.3	Efflux pump
ompA	4.3	Porine
ompC	3.0	Porine
ompF	2.6	Porine
osmC	5.9	Peroxidase
Iron metabolism		
fur	3.5	Regulator
entA to *entF*[b]	4.8	Enterochelin synthesis
dps	8.2	Ferritin
iscS	5.0	Cysteine desulfurase
sufS	4.5	Cysteine desulfurase
fpr	6.7	NADP:ferredoxin OR
Oxidative-stress resistance		
sodA	2.6	Superoxide dismutase
sodB	4.8	Superoxide dismutase
katE	2.0	Catalase
katG	4.6	Catalase
ahpCF[b]	2.5	Alkylhydroperoxide reductase
tpx	3.1	Peroxidase
bcp	2.5	Peroxidase
trxB	1.9	Thioredoxin reductase
trxA	2.4	Thioredoxin 1
trxC	6.0	Thioredoxin 2
gor	1.9	Glutathione reductase
grxB	3.5	Glutaredoxin 2
zwf	1.8	G6PDH
lpdA	2.3	Lipoamide dehydrogenase
DNA metabolism		
polB	6.0	Translesion polymerase
dinB	5.2	Translesion polymerase
uvrA to *uvrD*[b]	4.1	Nucleotide excision repair
mutS	3.7	Mismatch repair
recA	3.5	Recombinase
lexA	3.4	SOS response regulator
sulA	4.5	Cell division inhibitor
hns	2.8	Histone-like protein HNS
hupAB	3.3	Histone-like protein HU
RNA metabolism		
rpoD	1.2	Sigma 70 (housekeeping)
rpoH	2.4	Sigma 32 (heat)
rpoE	4.2	Sigma 24 (heat)
rpoS	3.9	Sigma S (multiple stresses)
rpoN	3.2	Sigma N (nitrogen metabolism)
cspA	1.9	Cold shock protein
cspB	2.2	Cold shock protein
cspE	7.4	Cold shock protein
cspF	3.2	Cold shock protein
cspG	2.5	Cold shock protein
ffs	2.5	4.5S RNA
ssrA	1.9	tmRNA
ssrS1	2.6	6S RNA
gcvB	8.0	GcvB RNA

[a] Gene transcription was analyzed using oligonucleotide arrays, as described in Materials and Methods. Gene expression ratios between the *yajL* mutant and the parental strain are shown. *P* values associated with the overexpression in the *yajL* mutant of genes involved in the different functions (chaperones/proteases/peptidases, chemical chaperones/osmotic stress, iron metabolism, oxidative-stress resistance, DNA metabolism [SOS regulation], and RNA metabolism) were highly significant (less than 10^{-4}).

[b] The mean value of the expression ratios for each gene is given.

creased expression of stress proteins and improved biochemical function.

Chaperones and proteases. Molecular chaperones prevent the aggregation of proteins and promote their efficient folding, whereas proteases degrade misfolded proteins that cannot be refolded. Some chaperones and proteases are expressed constitutively, but many of them are overexpressed upon environmental or protein stresses (42, 43). Several chaperones were 1.9- to 2.5-fold upregulated in the *yajL* mutant compared with their levels in the parental strain. These included the DnaK-DnaJ-GrpE chaperone machine, which is a central player in protein folding and solubilization; the disaggregating chaperone ClpB; and the nascent chain-associated protein trigger factor (Table 1). In contrast, the folding chaperone GroEL/GroES and the small heat shock proteins IbpA and IbpB were expressed at normal levels (data not shown). Several proteases and their associated chaperones (Lon, ClpA, ClpX, ClpP, and FtsH) and several peptidases (PepP, PepD, PepN, and PepQ) were 2- to 6-fold overexpressed in the *yajL* mutant (Table 1). We measured GroEL, DnaK, and ClpB levels in the *yajL* mutant by immunoblotting bacterial extracts with anti-GroEL, anti-DnaK, and anti-ClpB antibodies: whereas GroEL was expressed at slightly lower levels in the mutant (mutant/parental strain ratio, 0.8), DnaK and ClpB were overexpressed 1.8-fold and 2.5-fold, respectively, in accordance with the increased expression of their mRNAs (Fig. 1A).

Since unfolded proteins act as intracellular signals for induction of the heat shock response (42, 43), the overexpression of chaperones, proteases, and peptidases in the *yajL* mutant likely results from its protein oxidation and aggregation defects (9, 20)

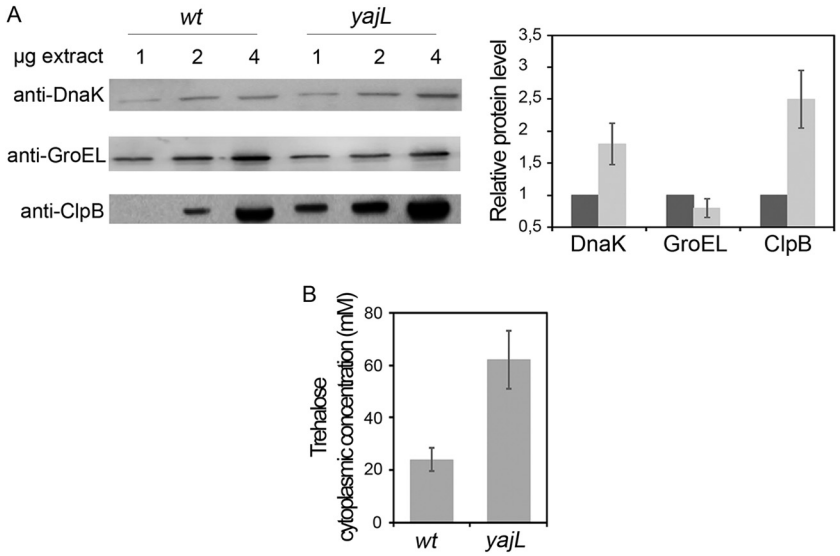

FIG 1 Levels of chaperones and chemical chaperones. (A) DnaK, GroEL, and ClpB levels. Extracts from the *yajL* mutant and the parental strain (wild type [wt]) were probed with anti-DnaK, anti-GroEL, and anti-ClpB antibodies, and protein amounts in the wild-type strain (black bars) and the *yajL* mutant (gray bars) were quantified by using ImageJ software (right). The data represent the means of three independent experiments. (B) Trehalose pools. Perchloric extracts from the *yajL* mutant and the parental strain (after exponential growth in LB medium containing 0.3 M NaCl) were analyzed for trehalose content. The data represent the means of three independent experiments. The error bars represent standard deviations.

and is probably mediated by the overexpression of sigma 32, the main regulator of the *E. coli* unfolded-protein response (see below). Overexpression of trigger factor in the *yajL* mutant may be linked to its ribosomal and translation accuracy defects (44). The clear results showing overexpression of chaperones and proteases in the *yajL* mutant contrast with contradictory results obtained in Parkinson's cells (24, 25, 45) and are in accordance with the protein aggregation phenotype of this mutant (9, 20, 21).

Osmotic-stress proteins and chemical chaperones. Bacteria and plants accumulate osmocompatible solutes (e.g., glycine betaine, proline, trimethylamine, trehalose, and glycerol) in response to salt stress or desiccation (46). Accumulation of osmoprotectants, however, is also induced by various environmental stresses and in stationary phase. Moreover, osmocompatible solutes function as chemical chaperones and prevent protein denaturation by stabilizing their native state. Trehalose protects yeast cells against heat and oxidative stresses (47), glycerol and trimethylamine prevent formation of the pathogenic scrapie prion protein in mouse neuroblastoma cells (48), and proline and glycine betaine confer thermotolerance on *E. coli dnaK* mutants (49, 50). Genes coding for the proline and glycine betaine transporters ProP and ProVWX, and for the trehalose synthesis enzymes OtsA and OtsB, were severalfold overexpressed in the *yajL* mutant, suggesting that chemical chaperones may be used by the mutant to alleviate its protein stress (Table 1). We measured the trehalose pools of the *yajL* mutant and the parental strain after exponential growth in LB medium containing 0.3 M NaCl and found that the trehalose concentration was severalfold higher in the mutant (62 mM, a concentration sufficient to reduce protein aggregation [51]) than in the parental strain (24 mM) (Fig. 1B).

Genes coding for the multidrug efflux pump AcrA-AcrB-TolC were also overexpressed (Table 1), suggesting that hydrophobic compounds induce the efflux pump in the mutant (52). Fatty acids and bile salts are known inducers of AcrAB (50), and defects in lipid and/or membrane metabolism in the *yajL* mutant might result in AcrAB induction. Hydrophobic peptides generated by protein degradation (4) might be inducers and substrates of the efflux pump, as well.

The outer membrane protein OsmC (a peroxidase for organic hydroperoxides) was 4.8-fold overexpressed in the *yajL* mutant, and porins OmpA, OmpC, and OmpF (required for peptide assimilation [53]) were also overexpressed (Table 1). The induction of these porins might be related to the nitrogen assimilation defect of the *yajL* mutant (V. Gautier, N. Messaoudi, J. Dairou, and G. Richarme, unpublished data). The overexpression of sigma S in the *yajL* mutant (see below) likely mediates the upregulation of several osmotic-stress genes (*proP*, *proVWX*, *otsA*, *otsB*, and *osmC* are controlled by sigma S [54]). The upregulation of genes coding for chemical chaperones and the activation of hydrophobic compound efflux systems in the *yajL* mutant suggests that this mutant uses a variety of mechanisms to alleviate its protein aggregation defect (9, 20, 21).

Oxidative stress. Oxidative stress is a hallmark of protein aggregation diseases, including Alzheimer's and Parkinson's diseases (5), and both *DJ-1* and *yajL* mutants are hypersensitive to oxidative stress (5, 9, 20). Genes coding for reactive oxygen species (ROS)-scavenging enzymes were 2- to 5-fold overexpressed in the *yajL* mutant, including those coding for superoxide dismutases SodA and SodB; catalases KatE and KatG; and peroxidases AhpCF, Tpx, and Bcp (Table 1). Several genes coding for protein oxidoreductases (55, 56) were 2- to 6-fold overexpressed, including those coding for thioredoxin reductase, thioredoxin 1, thioredoxin 2, and glutaredoxin 2. Other overexpressed genes coded for glucose-6-phosphate dehydrogenase, glutathione reductase, and lipoamide dehydrogenase. Oxidative-stress genes involved in tolerance for DNA damage (57) were also overexpressed (see "DNA metabolism" below).

We measured the expression of oxidative-stress genes in the

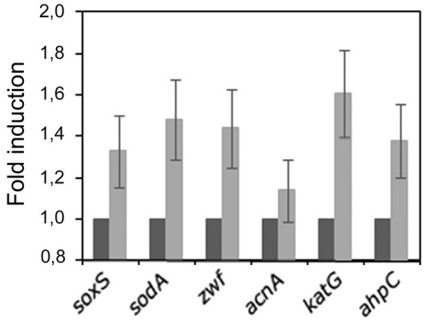

FIG 2 Expression of oxidative-stress probes. Expression of green fluorescent protein reporters for *soxS*, *sodA*, *zwf*, *acnA*, *katG*, and *ahpC* in the wild-type strain (black bars) and the *yajL* mutant (gray bars) was quantified by measuring the GFP fluorescence of cells (grown to exponential phase in LB medium) with a Hitachi spectrofluorimeter (excitation at 395 nm; emission at 509 nm). Gene expression values in the parental strain were normalized to 1. The data represent the means of three independent experiments. The error bars represent standard deviations.

yajL mutant by using translational fusions between *soxS*, *sodA*, *zwf*, *acnA*, *katG*, *ahpC*, and the gene coding for green fluorescent protein (35). Expression of *soxS* (transcriptional regulator of the SoxRS oxidative-stress regulon), *sodA* (superoxide dismutase SodA), *zwf* (glucose-6-phosphate dehydrogenase), *acnA* (aconitase A), *katG* (catalase KatG), and *ahpC* (alkylhydroperoxide reductase AhpC) was 1.2- to 1.7-fold higher in the *yajL* mutant than in the parental strain (Fig. 2). By using an in-gel assay (40), we measured the superoxide dismutase activities of the *yajL* mutant and found that SodA and SodB were 1.2- and 1.7-fold more active, respectively, than in the parental strain (Fig. 3B). We reported previously that the hydrogen peroxide pool was smaller in the *yajL* mutant (0.22 μM) than in the parental strain (0.27 μM) (9), and we show in Fig. 3A that the mutant is as efficient as the parental strain in detoxifying hydrogen peroxide. In contrast, as previously reported (39), the *katE katG ahpC* mutant (deficient in catalases KatE and KatG and in alkylhydroperoxide reductase AhpC) was severely impaired in hydrogen peroxide detoxification (Fig. 3A). Total glutathione levels were slightly higher in the mutant than in the parental strain (9.6 mM and 8.1 mM, respectively), and GSH/GSSG ratios were similar in both strains (285 and 305, respectively) (Fig. 3C), suggesting that, in contrast to the contradictory results reported for DJ-1 mutants (6, 19), the endogenous oxidative stress observed in the *yajL* mutant does not result from defects in glutathione metabolism. Overexpression of genes coding for ROS-scavenging enzymes and protein oxidoreductases in the *yajL* mutant may explain its low hydrogen peroxide levels (9) and its normal glutathione (this study) and protein dithiol/disulfide redox states (20). Despite its low hydrogen peroxide levels, the *yajL*

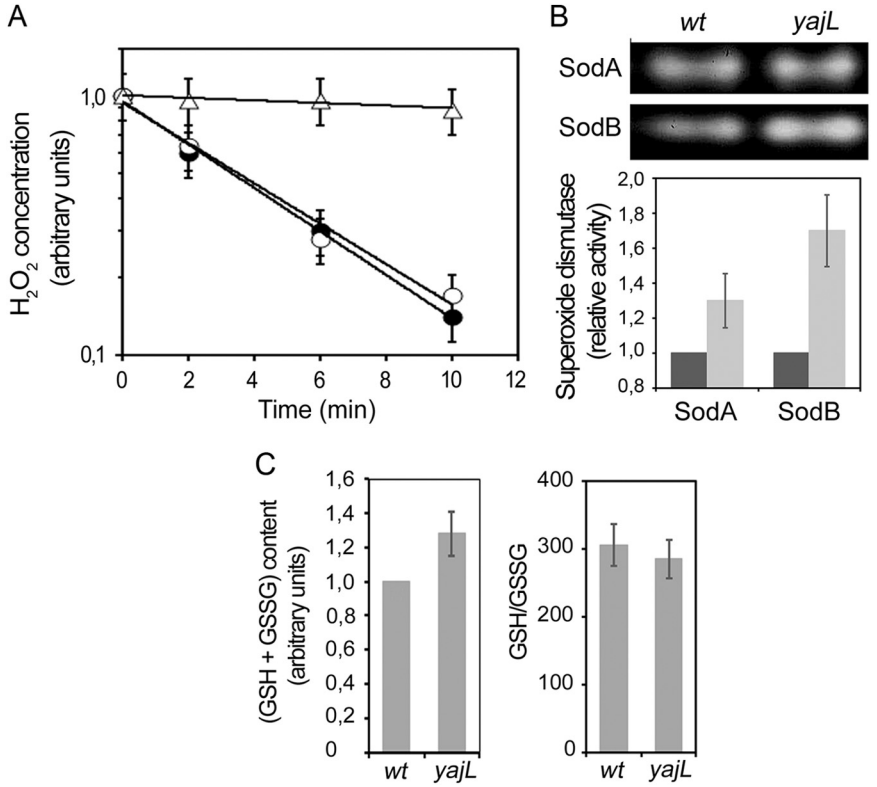

FIG 3 Hydrogen peroxide scavenging, superoxide dismutase activities, and glutathione pools. (A) Kinetics of 1.5 μM H_2O_2 decomposition by wt (solid circles), *yajL* (open circles), and *katE katG ahpC* (triangles) cells suspended in phosphate-buffered saline at an OD_{600} of 0.03. The data represent the means of three independent experiments. (B) SodA and SodB activities measured in crude bacterial extracts by the in-gel assay and quantified by using ImageJ software (bottom) (wild-type strain, black bars; *yajL* mutant, gray bars). Superoxide dismutase activities in the parental strain were normalized to 1. The data represent the means of four independent experiments. (C) GSH and GSSG levels were measured in bacterial perchloric acid extracts by using the glutathione reductase assay, as described in Materials and Methods. The arbitrary value of 1 represents an intracellular concentration of 9.6 mM. The data represent the means of three independent experiments. The error bars represent standard deviations.

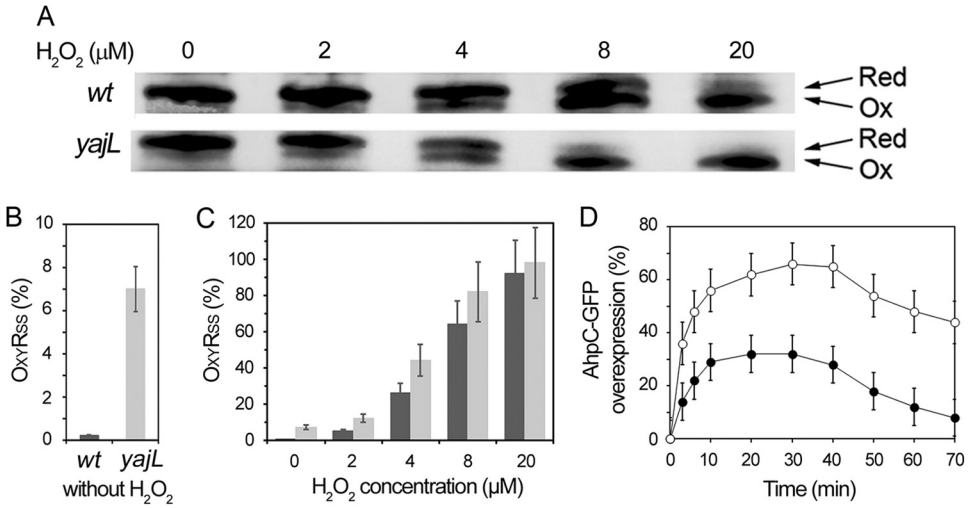

FIG 4 Disulfide bond formation in the oxidative-stress regulator OxyR. (A) Disulfide bond formation of OxyR, following exposure of bacteria to increasing hydrogen peroxide concentrations, was analyzed by SDS-PAGE. OxyR was detected with anti-OxyR antibodies. The oxidized (Ox) form of OxyR ($OxyR_{SS}$) migrates faster than the reduced (Red) form [$OxyR_{(SH)2}$]. (B and C) Protein amounts in the wild-type strain (black bars) and the *yajL* mutant (gray bars) were quantified by using ImageJ software and are represented at different hydrogen peroxide concentrations. The values are averages of the results of three independent experiments. (D) Hydrogen peroxide-induced overexpression of the AhpC-GFP reporter in the *yajL* mutant (open symbols) and the parental strain (solid symbols) after a 10-min exposure to 1 mM hydrogen peroxide (hydrogen peroxide was added to bacteria growing in LB medium at time zero and eliminated after 10 min by centrifugation and resuspension of bacteria in fresh LB medium). The data represent the means of three independent experiments. The error bars represent standard deviations.

mutant undergoes inactivation of several FeS enzymes, including aconitase B and NADH dehydrogenase I, probably because the covalent chaperone activity of YajL is absent in the mutant (20, 21).

To explain the induction of the oxidative-stress response in the *yajL* mutant, we investigated the redox state of its oxidative-stress regulator OxyR (OxyR is activated upon oxidative stress by cysteine 199 sulfenylation and disulfide formation between C199 and C208) (38). Bacteria were incubated in the absence or in the presence of hydrogen peroxide and immediately treated with TCA; proteins were separated by SDS-PAGE, transferred to nitrocellulose, and probed with anti-OxyR antibodies. In the absence of hydrogen peroxide, a significant amount of OxyR disulfide (around 7%) was detected in the mutant, but not in the parental strain (Fig. 4A and B); OxyR oxidation increased with increasing hydrogen peroxide concentrations and occurred at lower hydrogen peroxide concentrations in the mutant than in the parental strain (Fig. 4A and C). (Since the *yajL* mutant has low hydrogen peroxide levels [9], its basal increase in OxyR disulfide formation cannot be attributed to high hydrogen peroxide levels. It likely results from increased OxyR sulfenylation; increase in protein sulfenylation has been reported in the *yajL* mutant [20], as well as conversion of the sulfenylated form to the disulfide form.)

To confirm the role of YajL in the OxyR-regulated stress response, we measured the expression kinetics of the *ahpC-ahpGFP* reporter (OxyR regulated) after exposure to 1 mM hydrogen peroxide stress for 10 min. As shown in Fig. 4D, overexpression of AhpC-AhpGFP was greater in the *yajL* mutant than in the parental strain and lasted for longer after the stress had abated. This suggests that the *yajL* mutation affects both the efficiency and the kinetics of the oxidative-stress response by favoring the formation and durability of transcriptionally active forms of OxyR (e.g., sulfenyl and disulfide species).

Since full OxyR oxidation triggers a 5- to 50-fold overexpression of genes under its control (58, 59), the 7% basal oxidation in the *yajL* mutant may explain the 1.5- to 8-fold upregulation of OxyR target genes (*katG*, *ahpC*, *ahpF*, *trxC*, *gor*, *dps*, *fur*, and *sufS*). Moreover, the overexpression of *soxS*, *sodA*, *zwf*, *fpr*, and *acnA* (regulator and members of the SoxRS regulon, respectively) reported above suggests that the SoxRS regulon is also activated in the *yajL* mutant. Overexpression of several oxidative-stress genes in the mutant may also result from sigma S overexpression (see below), since *katE*, *katG*, *gor*, *dps*, and *sufS* are sigma S inducible (54). Thus, the three main regulators of the oxidative-stress response are activated (OxyR) or overexpressed (SoxS and sigma S) in the *yajL* mutant, resulting in the overexpression of many oxidative-stress genes.

Iron metabolism. Iron metabolism and oxidative stress are closely linked, especially because FeS clusters are particularly sensitive to reactive oxygen species and ferrous iron catalyzes hydroxyl radical formation via the Fenton reaction (58, 60). Many genes involved in iron metabolism were overexpressed in the *yajL* mutant, such as genes coding for synthesis of the enterochelin siderophore (*entABCDEF*) (Table 1). The ferritin Dps was 8-fold overexpressed, whereas ferritins Bfr, FtnA, and FtnB were expressed at normal levels (not shown). IscS and SufS, two cysteine desulfurases involved in FeS cluster biogenesis, and the ferredoxin-NADP reductase Fpr (also involved in FeS cluster biogenesis) were severalfold overexpressed, as was the global iron-dependent transcriptional regulator Fur. Thus, the *yajL* mutant overexpresses genes involved in iron acquisition and FeS cluster biogenesis. Since FeS protein defects have been reported to trigger overexpression of iron transporters and cysteine desulfurases (61), the occurrence of such defects in the *yajL* mutant (in which aconitase B and NADH dehydrogenase I are almost inactive [21]) may explain the overexpression of iron metabolism genes. Overexpression of the DNA-binding protein Dps (62) may contribute to

DNA protection (see below). Thus, FeS protein defects resulting from the YajL deficiency (20, 21) might be responsible for the induction of the iron stress response of the *yajL* mutant.

The activation of the iron stress response in the *yajL* mutant points to defects in iron metabolism (as evidenced by aconitase B and NADH dehydrogenase deficiencies [21] and the occurrence of many FeS proteins as YajL covalent partners [21]) and suggests that iron metabolism defects might be underestimated in Parkinson's cells.

DNA metabolism. Bacteria respond to DNA damage and defects in DNA replication, recombination, or repair by inducing the SOS response, which stimulates DNA repair and translesion DNA synthesis (57). Translesion DNA polymerases 2 (PolB) and 4 (DinB) were severalfold overexpressed in the mutant (Table 1), as were several genes involved in DNA repair, including *mutS* (mismatch repair), *uvrABCD* (nucleotide excision repair), and *recA*. Genes coding for base excision repair (*mutM*, *nth*, *nei*, *alka*, *mutY*, *nfo*, and *xth*) were expresssed at normal levels (not shown), whereas genes coding for the cell division inhibitor SulA and the SOS response regulator LexA were overexpressed. Histone-like proteins were also overexpressed, including HNS, which plays a key role in transcriptional regulation and chromosomal organization (63), and HU-alpha and HU-beta, which are involved in transcriptional regulation and nucleoid compaction.

Induction of the SOS response led us to check whether DNA damage was increased in the *yajL* mutant, by using the DNA damage apurinic-site-counting kit and by measuring the rate of mutation to rifampin resistance. The numbers of apurinic sites were similar between the *yajL* mutant and the parental strain (13 ± 1 per 100,000 bp in both strains [data not shown]), as was the mutation frequency (around 5 rifampin-resistant mutants per 10^8 cells for both strains [data not shown]), which suggests either that the *yajL* mutant displays levels of DNA damage similar to those of the parental strain or that it suffers slightly higher levels of DNA damage that are erased by DNA repair processes. The induction of the SOS response in the *yajL* mutant, in the absence of a measurable increase in DNA damage, suggests that the SOS response was induced by defects in DNA metabolism enzymes (see Discussion). This would corroborate the prevalence of protein defects in this mutant (9, 20, 21) and in DJ-1-associated Parkinson cells.

Stress sigma factors, RNA chaperones, and small stable RNAs. Transcription in *E. coli* involves RNA polymerase and multiple interchangeable sigma factors, each of which recognizes a single set of promoters. Sigma 70 is involved in the transcription of most genes in growing cells, whereas several specialized sigma factors are involved in the transcription of stress response genes and in transcription during the stationary phase (64). The gene *rpoD* (encoding sigma 70) was expressed at normal levels in the *yajL* mutant, whereas mRNAs coding for heat stress, extracytoplasmic stress, multistress, and nitrogen stress sigma factors (sigma 32/RpoH, sigma 24/RpoE, sigma S/RpoS, and sigma 54/RpoN, respectively) were 2- to 4-fold overexpressed (Table 1).

We measured by immunodetection the expression of sigma 70, sigma S, and sigma 32 in the *yajL* mutant. Sigma 70 was expressed at similar levels in both strains (Fig. 5A). The level of sigma 32 at 30°C was 1.5-fold higher in the *yajL* mutant than in the parental strain and was increased severalfold in both strains after heat shock at 42°C (Fig. 5B). During the exponential phase, sigma S was hardly detectable in the parental strain, as previously reported (37, 54), but was expressed at significant levels in the *yajL* mutant (Fig. 5C) (in stationary phase, sigma S was overexpressed at similar levels in both strains [data not shown]). Since sigma S levels depend on its stability, we measured its half-life in exponential-phase bacteria. The half-life of sigma S increased from around 60 s in the parental strain (as previously reported [37, 54]) to 110 s in the mutant (Fig. 5D), suggesting that both increased mRNA levels and protein stability contribute to its overexpression in the mutant. The increased levels and stability of sigma S in the *yajL* mutant may result from its protein aggregation phenotype (see Discussion) (65).

Genes coding for the RNA chaperones CspA, CspB, CspE, CspF, and CspG were up to 7-fold overexpressed in the *yajL* mutant. Since the *yajL* mutant displays mRNA expression defects (9), translational frameshifting, and increased dissociation of 70S monosomes (44), it may require increased amounts of RNA chaperones, which destabilize RNA secondary structures and favor transcription, translation, and ribosome assembly (66). In addition to their involvement in cold adaptation, CspA family proteins play important roles in recovery from nutritional stress, chromosome condensation, and mRNA decay and expression of stress proteins by stabilizing the *rpoS* mRNA (67), suggesting that their overexpression could affect multiple functions in the cell.

Several noncoding regulatory RNAs (68) were overexpressed in the *yajL* mutant, including 4.5S RNA (the RNA component of the signal recognition particle), 6S RNA (which down- and up-regulates sigma 70- and sigma S-dependent transcription, respectively), transfer-messenger RNA (tmRNA) (ribosome rescue and increased translation accuracy), and GcvB (amino acid metabolism regulation). Overexpression of 6S RNA, tmRNA, and GcvB in the *yajL* mutant could be related to its increased expression of sigma S-dependent genes (this study), translational defects (9, 44), and amino acid metabolism defects (Gautier et al., unpublished), respectively.

Thus, the *yajL* mutant regulates its global stress response by using RNA polymerase sigma factors (principally sigma 32 and sigma S), transcription factors (OxyR and SoxRS), RNA chaperones (CspA family proteins), and small regulatory RNAs (6S RNA, tmRNA, and GcvB).

Peptidoglycan synthesis. *E. coli* cells elongate via the incorporation of peptidoglycan precursors by elongation-specific murein synthesis complexes (PBP2, PBP1A, MreC, MreD, RodA, RodZ, and LpoA) at filaments of the actin-like MreB and septate via the incorporation of peptidoglycan precursors by cell division-specific murein synthesis complexes (PBP3, PBP1B, FtsN, FtsW, FtsZ, ZipA, FtsQ, FtsL, FtsB, FtsK, FtsA, FtsE, FtsX, and LpoB) at the tubulin-like FtsZ ring (69, 70). Under stress, or at the onset of stationary phase, bacteria adopt a shorter and rounder shape by switching from cell elongation to septation systems (69, 70). In the *yajL* mutant, genes involved in peptidoglycan elongation were globally underexpressed, whereas those involved in septation were globally overexpressed (Fig. 6). The shapes of the cells of the *yajL* mutant and parental strains were investigated by using phase-contrast microscopy. Parental cells exhibited a normal rod shape at midexponential phase ($OD_{600} = 0.2$), whereas the *yajL* mutant displayed many short rods and oval cells (Fig. 6) (both parental and mutant cells were short rods or oval in stationary phase [data not shown]). This result suggests that the *yajL* mutant adopts a shorter and rounder shape as part of its strategy to compensate for YajL deficiency.

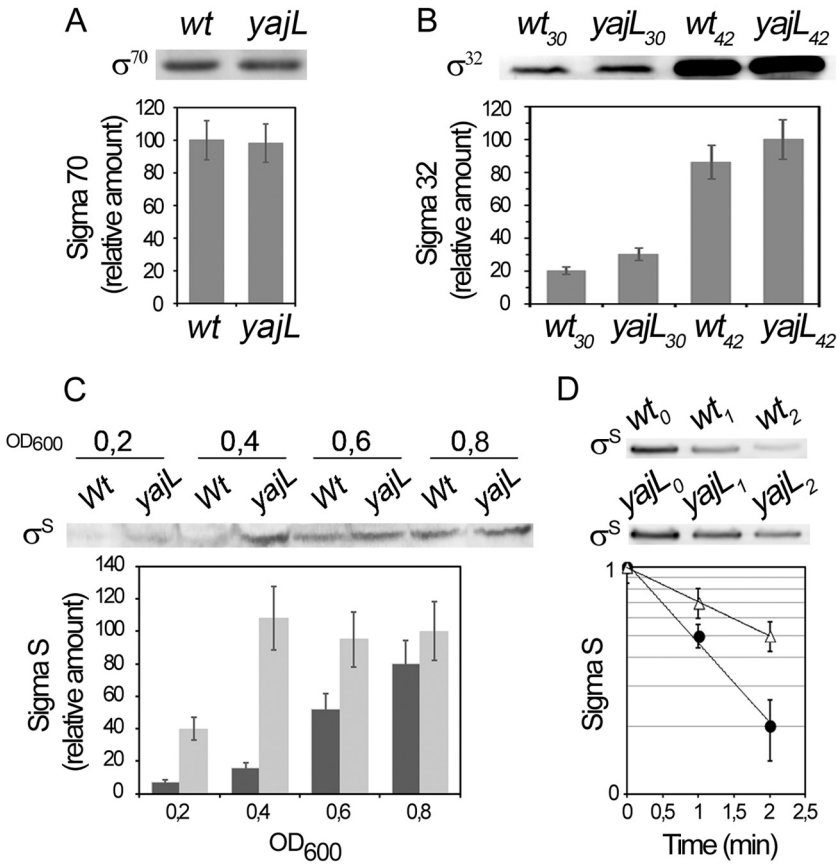

FIG 5 Sigma 70, sigma 32, and sigma S levels in the *yajL* mutant. Bacteria were treated with 10% TCA, and resolubilized proteins were probed with anti-sigma 70 (A), anti-sigma 32 (bacteria were harvested after growth at 30°C or after heat shock for 5 min at 42°C) (B), and anti-sigma S (bacteria were harvested in exponential phase at different OD_{600} values) (C) antibodies, and protein amounts in the wild-type strain (black bars) and the *yajL* mutant (gray bars) were quantified by using ImageJ software. The data represent the means of three independent experiments. (D) Sigma S stability. Bacteria in exponential phase (OD_{600} = 0.3) were treated with 100 μg/ml chloramphenicol, and sigma S levels were determined at several times with anti-sigma S antibodies (the amount of wt cells used for immunodetection was 5-fold higher than that of *yajL* mutant cells). Sigma S amounts in wt (circles) and *yajL* mutant (triangles) cells were quantified by using ImageJ software and are represented (in logarithmic scale) as a function of time after chloramphenicol addition. The data represent the means of three independent experiments. The error bars represent standard deviations.

DISCUSSION

In this work, we show that the *yajL* mutation triggers the onset of a global stress response that consists of the overexpression of genes coding for chaperones, proteases, chemical chaperone transporters, superoxide dismutases, catalases, peroxidases, components of thioredoxin and glutaredoxin systems, iron transporters, ferritins and FeS cluster biogenesis enzymes, DNA repair proteins, RNA chaperones, and small regulatory RNAs, and also those involved in peptidoglycan septation.

Chaperones, peptidases, chemical chaperones, and efflux pump. The DnaK chaperone machine and the disaggregase ClpB help the *yajL* mutant to resolve its protein aggregation defects (9, 42, 43), and chemical chaperones may contribute to protein solubilization (5, 49, 50). Overexpressed proteases (Lon, Clp, and FtsH) and peptidases favor the degradation of protein aggregates (42, 43, 71), and the efflux pump AcrAB may discard aggregation-prone hydrophobic peptides (52, 72). Thus, the *yajL* mutant sets up a coherent protein stress response to cope with protein aggregation.

In eukaryotic cells, Hsp70 and Hsp40 (DnaK and DnaJ counterparts) have been extensively implicated in the pathogenesis of protein-misfolding diseases, and their overexpression reduces the aggregation and toxicity of Aβ peptides and α-synuclein (73, 74). Moreover, the yeast disaggregase Hsp104 (a ClpB counterpart), when overexpressed in mammalian cell lines, inhibits Aβ amyloidogenesis and reverses the formation of α-synuclein fibers (75). Hsp70 and/or Hsp40 has been reported to be either overexpressed (23–25) or underexpressed (24, 45) in Parkinsonism, and Hsp70 is upregulated in the presence of DJ-1 (76). Protein degradation defects are also involved in protein aggregation diseases (71, 77): the Parkinsonism-associated protein parkin is an E3 ubiquitin ligase (5), and ubiquitin-conjugating enzymes and proteasome subunits are downregulated in several forms of Parkinsonism (24, 45).

As for chemical chaperones, they are not synthesized by mammalian cells, but they have been used to correct prion and synuclein folding defects (48, 78). The function of the AcrAB efflux pump is reminiscent of that of the eukaryotic multidrug resistance P glycoprotein, which expels beta-amyloid peptides (72), and of that of glutathione *S*-transferases, which play a role in detoxification and are upregulated in several forms of Parkinsonism (25, 26), including in DJ-1-deficient cells (25).

Oxidative-stress resistance and iron metabolism. Overex-

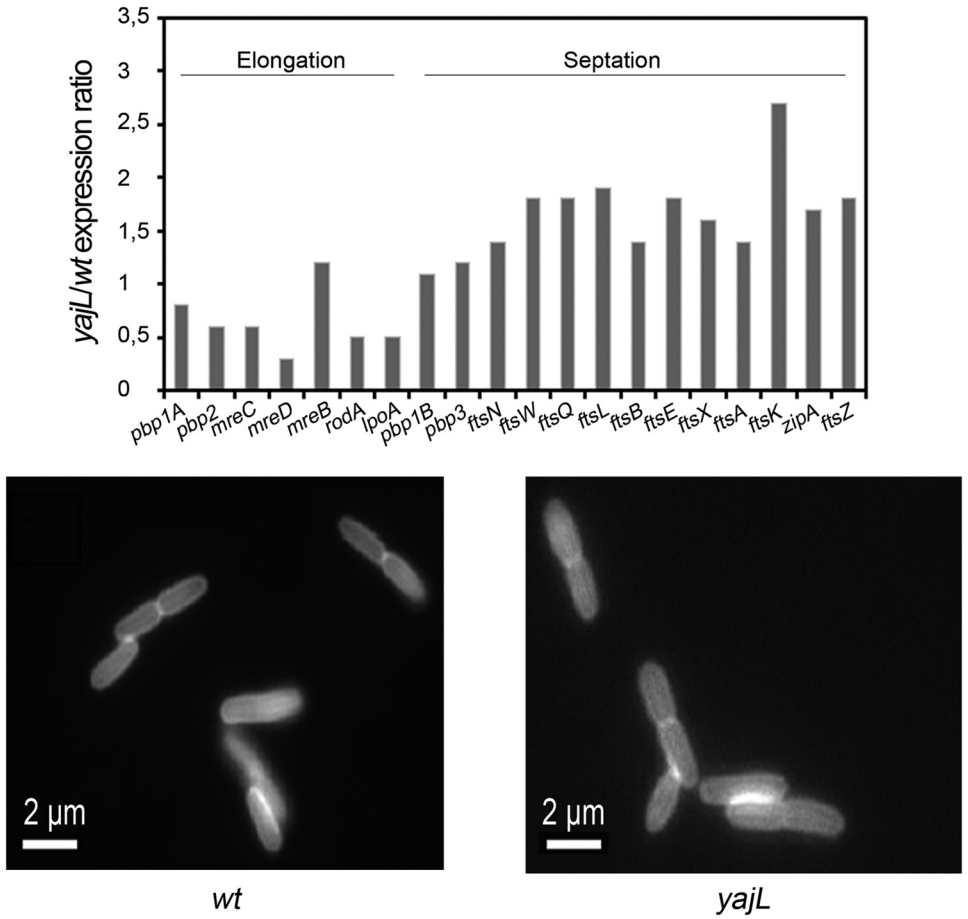

FIG 6 Expression of peptidoglycan synthesis genes and microscopic observation of bacteria. (A) Expression of genes coding for elongation-specific and cell division-specific peptidoglycan synthesis complexes. (B) Microscopic observation of bacterial cells. Shown are fluorescence images of wild-type and *yajL* mutant cells labeled with the membrane-binding fluorescent dye FM4-64.

pressed ROS-scavenging enzymes, thioredoxin/glutaredoxin systems, and NADPH-producing enzymes in the *yajL* mutant help lower hydrogen peroxide levels (9), maintain a normal protein dithiol-disulfide redox state (9, 21), and restrict protein oxidation to acceptable levels (20, 55). Despite its oxidative-stress response, the *yajL* mutant displays protein sulfenylation and FeS protein defects (20, 21) that may trigger the upregulation of iron metabolism genes, including iron transporters, ferritins, and enzymes involved in FeS cluster biogenesis (61).

Gene expression profiling of DJ-1 knockdown cells underscored 49 overexpressed genes, including glutathione *S*-transferase (25) and many genes whose functions are thought to be related to cell death or neurodegeneration, but it was not possible to describe a coherent oxidative-stress response like that reported in the present study. In contrast, other studies reported that DJ-1 mutants are deficient in glutathione metabolism (6, 19) and cytoplasmic superoxide dismutase (79) and that levels of Nrf2 (the main eukaryotic oxidative-stress regulator) and of Nrf2-dependent genes are lowered (13) or unaffected by DJ-1 disruption (80).

FeS cluster defects have not been formally reported in DJ-1-deficient cells, although aconitase and complex I deficiencies have been described (12, 81). Interestingly, a 35% increase in iron content has been observed in the substantia nigra of Parkinson's patients, with an elevation of the Fe^{2+}/Fe^{3+} ratio and oxidative stress characterized by a lower GSH content, reduced catalase activity, higher superoxide dismutase activities, DNA oxidation, protein carbonylation, and FeS cluster biogenesis defects (82), suggesting that disturbances in iron metabolism occur in Parkinsonism.

Thus, in contrast to eukaryotic cells, the *yajL* mutant uses a clear strategy to compensate for its protein oxidation defect (9, 20, 21): it overproduces ROS-scavenging enzymes, protein oxidoreductases, and enzymes involved in glutathione metabolism (which explains its low hydrogen peroxide level and its normal glutathione level and redox state) to keep protein oxidation at acceptable levels. Moreover, its oxidative-stress response is powered by the oxidative-stress regulators OxyR and SoxRS and by sigma S.

SOS response and DNA metabolism. The *yajL* mutant induced a SOS response (57), although it did not display increased DNA damage. Since chronic SOS induction occurs in mutants defective in DNA repair, recombination, or replication genes and since several of these mutants (*lig*, *recN*, *ftsE*, *ftsX*, and *priA*) induce the SOS response without displaying a mutator phenotype (83), the induction of the SOS response in the *yajL* mutant may result from defects in DNA metabolism enzymes. It may also result from defective regulation by RecA/LexA: LexA does not con-

tain cysteine residues; however, cysteine 117 in RecA plays a role in the RecA-promoted cleavage of LexA (84). The possible oxidation of this residue in the *yajL* mutant might result in increased cleavage of the LexA repressor. Moreover, several genes, such as *polB* and *dinB*, display sigma S-inducible expression: thus, overexpression of these genes in the *yajL* mutant might be due to the fact that it contains higher levels of sigma S.

To our knowledge, DJ-1-deficient cells have not been reported to undergo DNA damage. However, the Parkinsonism-associated parkin protects mitochondrial DNA from damage caused by oxidative stress (83), and increased 8-oxoguanine levels have been detected in mitochondria in the substantia nigra of Parkinson's patients (84), suggesting that DNA damage may occur in Parkinsonism.

Stress sigma factors and RNA metabolism. The *yajL* mutant overexpressed stress sigma factors (sigma 24, sigma 32, sigma 54, and sigma S), which contribute to induction of the stress response (54). It also overexpressed RNA chaperones and small regulatory RNAs, which are involved in upregulating stress genes (6S RNA) and in preventing defects in translation (RNA chaperones and tmRNA) and metabolism (GcvB RNA) (66, 68). The stabilization of sigma S in the *yajL* mutant (which accumulates both oxidized and aggregated proteins [9, 20, 21] and displays decreased translational accuracy [44]) is reminiscent of its stabilization in ribosomal inaccurate mutants, which accumulate oxidatively modified aberrant proteins (65). In contrast, the similar growth rates shown by the *yajL* mutant and the parental strain (unpublished results) suggest that they contain similar ppGpp pools (54). This disfavors ppGpp as a contributor to the higher sigma S levels observed in the *yajL* mutant (ppGpp stimulates *rpoS* transcription, as well as the formation of the RpoS-RNA polymerase holoenzyme, which activates RpoS and protects it against degradation). Overexpression of sigma 32 likely mediates the upregulation of chaperones, proteases, and peptidases, and overexpression of sigma S mediates the upregulation of several osmotic- and oxidative-stress genes. Overexpression of sigma 54 in the mutant may be caused by its amino acid utilization defect (Gautier et al., unpublished). As stated above, DJ-1 does not upregulate the oxidative-stress transcription factor Nrf2 (13, 80) but regulates gene expression at the translational level by binding, in an oxidation-dependent manner, multiple RNA targets coding for selenoproteins, glutathione peroxidases, NADH dehydrogenase, and cytochrome oxidase (15, 16).

To sum up, the global stress response of the *yajL* mutant is mainly mediated by its protein stress (protein sulfenylation, protein aggregation, and FeS protein defects [9, 20, 21]), which results in the upregulation of sigma 32 and sigma S (42, 43, 54), the upregulation of the oxidative-stress regulator SoxS, and the activation of the oxidative-stress regulator OxyR (activated by sulfenylation and disulfidation). Protein defects of this mutant may also activate the iron stress response (inducible by FeS protein defects [61]) and the SOS response (inducible by defects in replication enzymes [83] or in LexA/RecA [57, 84]).

Peptidoglycan synthesis. Like stressed cells and stationary-phase cells, the *yajL* mutant adopts a shorter and rounder shape, causing a decrease in the surface-to-volume ratio and a reduction in the surface area exposed to the environment. Such shorter and rounder *E. coli* cells are frequently observed under environmental-stress conditions (69, 70, 85). Thus, the adoption of a shorter and rounder shape by the *yajL* mutant is part of its strategy to compensate for YajL deficiency.

Stress response of Parkinson's disease brain tissue. Taken together, genome-wide expression studies of the Parkinson's disease brain suggest that stress responses are involved in the disease (22), but none of these studies revealed a global stress response such as that reported in our prokaryotic model of DJ-1-associated Parkinsonism (22). Other studies show that overexpression of Hsp70 and Hsp40 (24, 25) contrasts with the downregulation of Hsp105, Hsp90, Hsp70, Hsp40, and Hsp10 (45). Similarly, the upregulation of glutathione *S*-transferase (25, 26) and of superoxide dismutase (12) contrasts with the downregulation of glutathione *S*-transferase M3 (26), superoxide dismutase (25, 79), and Nrf2 (13). Thus, increases in stress gene expression reported in some studies are frequently contradicted by decreases reported in others. In a more consensual manner, FeS protein defects (2, 81, 82) and the activation of iron metabolism have been reported in many studies (22), as well as DNA damage (86, 87) and induction of DNA repair enzymes (23, 25). The contradictory results may be explained by problems inherent in genome-wide expression studies of Parkinson's disease brain tissues, such as a mixed cell population with the presence of dying cells, elapsed time between death and freezing of brain tissue, brain anoxic states, and the fact that most gene expression changes may represent downstream consequences of a disease whose onset occurred many years before the gene expression analysis.

Finally, the great similarity betweeen protein insults and stress responses in prokaryotes and eukaryotes and the clarity of the presently described stress response enhance the value of the present study (although one must be cautious when comparing prokaryotic and eukaryotic cells, in which YajL and DJ-1 may have different targets). Our results suggest, however, that a global stress response similar to that described here might occur during the early phase of DJ-1-associated Parkinsonism.

ACKNOWLEDGMENTS

This work was supported by program grant PHC-Utique 10G0803 (G. Richarme and N. Messaoudi), by a grant from the Fondation pour la Recherche Médicale to F. Kthiri, and by an EMBO short-term fellowship to M. Mihoub.

We thank Ivan Matic, Université Paris Descartes, INSERM Unit 1001, for helpful discussions and D. Krzysztof Liberek, Faculty of Biotechnology, Gdansk University, Poland, for providing us with anti-ClpB antibodies.

REFERENCES

1. **Quigley PM, Korotkov K, Baneyx F, Hol WG.** 2003. The 1.6-A crystal structure of the class of chaperones represented by *Escherichia coli* Hsp31 reveals a putative catalytic triad. Proc. Natl. Acad. Sci. U. S. A. **100**:3137–3142.
2. **Sastry MS, Korotkov K, Brodsky Y, Baneyx F.** 2002. Hsp31, the *Escherichia coli yedU* gene product, is a molecular chaperone whose activity is inhibited by ATP at high temperatures. J. Biol. Chem. **277**:46026–46034.
3. **Lee SJ, Kim SJ, Kim IK, Ko J, Jeong CS, Kim GH, Park C, Kang SO, Suh PG, Lee HS, Cha SS.** 2003. Crystal structures of human DJ-1 and *Escherichia coli* Hsp31, which share an evolutionarily conserved domain. J. Biol. Chem. **278**:44552–44559.
4. **Malki A, Caldas T, Abdallah J, Kern R, Eckey V, Kim SJ, Cha SS, Mori H, Richarme G.** 2005. Peptidase activity of the *Escherichia coli* Hsp31 chaperone. J. Biol. Chem. **280**:14420–14426.
5. **Cookson MR.** 2005. The biochemistry of Parkinson's disease. Annu. Rev. Biochem. **74**:29–52.
6. **Wilson MA.** 2011. The role of cysteine oxidation in DJ-1 function and dysfunction. Antioxid. Redox Signal. **15**:111–122.

7. **Wilson MA, Collins JL, Hod Y, Ringe D, Petsko GA.** 2003. The 1.1-A resolution crystal structure of DJ-1, the protein mutated in autosomal recessive early onset Parkinson's disease. Proc. Natl. Acad. Sci. U. S. A. **100**:9256–9261.
8. **Wilson MA, Ringe D, Petsko GA.** 2005. The atomic resolution crystal structure of the YajL (ThiJ) protein from *Escherichia coli*: a close prokaryotic homologue of the Parkinsonism-associated protein DJ-1. J. Mol. Biol. **353**:678–691.
9. **Kthiri F, Le HT, Gautier V, Caldas T, Malki A, Landoulsi A, Bohn C, Bouloc P, Richarme G.** 2010. Protein aggregation in a mutant deficient in YajL, the bacterial homolog of the Parkinsonism-associated protein DJ-1. J. Biol. Chem. **285**:10328–10336.
10. **Shendelman S, Jonason A, Martinat C, Leete T, Abeliovich A.** 2004. DJ-1 is a redox-dependent molecular chaperone that inhibits alpha-synuclein aggregate formation. PLoS Biol. **2**:e362. doi:10.1371/journal.pbio.0020362.
11. **Zhou W, Zhu M, Wilson MA, Petsko GA, Fink AL.** 2006. The oxidation state of DJ-1 regulates its chaperone activity toward alpha-synuclein. J. Mol. Biol. **356**:1036–1048.
12. **Andres-Mateos E, Perier C, Zhang L, Blanchard-Fillion B, Greco TM, Thomas B, Ko HS, Sasaki M, Ischiropoulos H, Przedborski S, Dawson TM, Dawson VL.** 2007. DJ-1 gene deletion reveals that DJ-1 is an atypical peroxiredoxin-like peroxidase. Proc. Natl. Acad. Sci. U. S. A. **104**:14807–14812.
13. **Clements CM, McNally RS, Conti BJ, Mak TW, Ting JP.** 2006. DJ-1, a cancer- and Parkinson's disease-associated protein, stabilizes the antioxidant transcriptional master regulator Nrf2. Proc. Natl. Acad. Sci. U. S. A. **103**:15091–15096.
14. **Junn E, Taniguchi H, Jeong BS, Zhao X, Ichijo H, Mouradian MM.** 2005. Interaction of DJ-1 with Daxx inhibits apoptosis signal-regulating kinase 1 activity and cell death. Proc. Natl. Acad. Sci. U. S. A. **102**:9691–9696.
15. **Blackinton J, Kumaran R, van der Brug MP, Ahmad R, Olson L, Galter D, Lees A, Bandopadhyay R, Cookson MR.** 2009. Post-transcriptional regulation of mRNA associated with DJ-1 in sporadic Parkinson disease. Neurosci. Lett. **452**:8–11.
16. **van der Brug MP, Blackinton J, Chandran J, Hao LY, Lal A, Mazan-Mamczarz K, Martindale J, Xie C, Ahmad R, Thomas KJ, Beilina A, Gibbs JR, Ding J, Myers AJ, Zhan M, Cai H, Bonini NM, Gorospe M, Cookson MR.** 2008. RNA binding activity of the recessive Parkinsonism protein DJ-1 supports involvement in multiple cellular pathways. Proc. Natl. Acad. Sci. U. S. A. **105**:10244–10249.
17. **Guzman JN, Sanchez-Padilla J, Wokosin D, Kondapalli J, Ilijic E, Schumacker PT, Surmeier DJ.** 2010. Oxidant stress evoked by pacemaking in dopaminergic neurons is attenuated by DJ-1. Nature **468**:696–700.
18. **Liu F, Nguyen JL, Hulleman JD, Li L, Rochet JC.** 2008. Mechanisms of DJ-1 neuroprotection in a cellular model of Parkinson's disease. J. Neurochem. **105**:2435–2453.
19. **Zhou W, Freed CR.** 2005. DJ-1 up-regulates glutathione synthesis during oxidative stress and inhibits A53T alpha-synuclein toxicity. J. Biol. Chem. **280**:43150–43158.
20. **Gautier V, Le HT, Malki A, Messaoudi N, Caldas T, Kthiri F, Landoulsi A, Richarme G.** 2012. YajL, the prokaryotic homolog of the parkinsonism-associated protein DJ-1, protects cells against protein sulfenylation. J. Mol. Biol. **421**:662–670.
21. **Le HT, Gautier V, Kthiri F, Malki A, Messaoudi N, Mihoub M, Landoulsi A, An YJ, Cha SS, Richarme G.** 2012. YajL, prokaryotic homolog of Parkinsonism-associated protein DJ-1, functions as a covalent chaperone for thiol proteome. J. Biol. Chem. **287**:5861–5870.
22. **Lewis PA, Cookson MR.** 2012. Gene expression in the Parkinson's disease brain. Brain Res. Bull. **88**:302–312.
23. **Grunblatt E, Mandel S, Jacob-Hirsch J, Zeligson S, Amariglo N, Rechavi G, Li J, Ravid R, Roggendorf W, Riederer P, Youdim MB.** 2004. Gene expression profiling of parkinsonian *substantia nigra* pars compacta; alterations in ubiquitin-proteasome, heat shock protein, iron and oxidative stress regulated proteins, cell adhesion/cellular matrix and vesicle trafficking genes. J. Neural Transm. **111**:1543–1573.
24. **Hauser MA, Li YJ, Xu H, Noureddine MA, Shao YS, Gullans SR, Scherzer CR, Jensen RV, McLaurin AC, Gibson JR, Scott BL, Jewett RM, Stenger JE, Schmechel DE, Hulette CM, Vance JM.** 2005. Expression profiling of substantia nigra in Parkinson disease, progressive supranuclear palsy, and frontotemporal dementia with parkinsonism. Arch. Neurol. **62**:917–921.
25. **Nishinaga H, Takahashi-Niki K, Taira T, Andreadis A, Iguchi-Ariga SM, Ariga H.** 2005. Expression profiles of genes in DJ-1-knockdown and L 166 P DJ-1 mutant cells. Neurosci. Lett. **390**:54–59.
26. **Miller RM, Kiser GL, Kaysser-Kranich TM, Lockner RJ, Palaniappan C, Federoff HJ.** 2006. Robust dysregulation of gene expression in *substantia nigra* and *striatum* in Parkinson's disease. Neurobiol Dis. **21**:305–313.
27. **Datsenko KA, Wanner BL.** 2000. One-step inactivation of chromosomal genes in *Escherichia coli* K-12 using PCR products. Proc. Natl. Acad. Sci. U. S. A. **97**:6640–6645.
28. **Yu D, Ellis HM, Lee EC, Jenkins NA, Copeland NG, Court DL.** 2000. An efficient recombination system for chromosome engineering in *Escherichia coli*. Proc. Natl. Acad. Sci. U. S. A. **97**:5978–5983.
29. **Bohn C, Collier J, Bouloc P.** 2004. Dispensable PDZ domain of *Escherichia coli* YaeL essential protease. Mol. Microbiol. **52**:427–435.
30. **Miller JH.** 1992. A short course in bacterial genetics. Cold Spring Harbor Laboratory, Cold Spring Harbor, NY.
31. **Collier J, Bohn C, Bouloc P.** 2004. SsrA tagging of *Escherichia coli* SecM at its translation arrest sequence. J. Biol. Chem. **279**:54193–54201.
32. **Quackenbush J.** 2002. Microarray data normalization and transformation. Nat. Genet. **32**:496–501.
33. **Boyle EI, Weng S, Gollub J, Bostein H, Cherry JM, Sherlock G.** 2004. GO::TermFinder open source software for accessing gene ontology information and finding significantly enriched gene ontology terms associated with a list of genes. Bioinformatics **20**:3710–3715.
34. **Lelandais G, Saint-Georges Y, Geneix C, Al-Shickley L, Dujardin G, Jacq C.** 2009. Spatio-temporal dynamics of yeast mitochondrial biogenesis: transcriptional and post-transcriptional mRNA oscillatory modules. PLoS Comput. Biol. **5**:e1000409. doi:10.1371/journal.pcbi.1000409.
35. **Lu C, Albano CR, Bentley WE, Rao G.** 2005. Quantitative and kinetic study of oxidative stress regulons using green fluorescent protein. Biotechnol. Bioeng. **89**:574–587.
36. **Lewandowska A, Matuszewska M, Liberek K.** 2007. Conformational properties of aggregated polypeptides determine ClpB-dependence in the disaggregation process. J. Mol. Biol. **371**:800–811.
37. **Lange R, Hengge-Aronis R.** 1994. The cellular concentration of the sigma S subunit of RNA polymerase in *Escherichia coli* is controlled at the levels of transcription, translation, and protein stability. Genes Dev. **8**:1600–1612.
38. **Tao K.** 1999. *In vivo* oxidation-reduction kinetics of OxyR, the transcriptional activator for an oxidative stress-inducible regulon in *Escherichia coli*. FEBS Lett. **457**:90–92.
39. **Seaver LC, Imlay JA.** 2001. Alkyl hydroperoxide reductase is the primary scavenger of endogenous hydrogen peroxide in *Escherichia coli*. J. Bacteriol. **183**:7173–7181.
40. **Beauchamp C, Fridovich I.** 1971. Superoxide dismutase: improved assays and an assay applicable to acrylamide gels. Anal. Biochem. **44**:276–287.
41. **Richarme G.** 1988. A novel aspect of the inhibition by arsenicals of binding-protein-dependent galactose transport in gram-negative bacteria. Biochem. J. **253**:371–376.
42. **Bukau B, Weissman J, Horwich A.** 2006. Molecular chaperones and protein quality control. Cell **125**:443–451.
43. **Parsell DA, Sauer RT.** 1989. Induction of a heat shock-like response by unfolded protein in *Escherichia coli*: dependence on protein level not protein degradation. Genes Dev. **3**:1226–1232.
44. **Kthiri F, Gautier V, Le HT, Prere MF, Fayet O, Malki A, Landoulsi A, Richarme G.** 2010. Translational defects in a mutant deficient in YajL, the bacterial homolog of the Parkinsonism-associated protein DJ-1. J. Bacteriol. **192**:6302–6306.
45. **Simunovic F, Yi M, Wang Y, Macey L, Brown LT, Krichevsky AM, Andersen SL, Stephens RM, Benes FM, Sonntag KC.** 2009. Gene expression profiling of *substantia nigra* dopamine neurons: further insights into Parkinson's disease pathology. Brain **132**:1795–1809.
46. **Kempf B, Bremer E.** 1998. Uptake and synthesis of compatible solutes as microbial stress responses to high-osmolality environments. Arch. Microbiol. **170**:319–330.
47. **Benaroudj N, Lee DH, Goldberg AL.** 2001. Trehalose accumulation during cellular stress protects cells and cellular proteins from damage by oxygen radicals. J. Biol. Chem. **276**:24261–24267.
48. **Tatzelt J, Prusiner SB, Welch WJ.** 1996. Chemical chaperones interfere with the formation of scrapie prion protein. EMBO J. **15**:6363–6373.
49. **Caldas T, Demont-Caulet N, Ghazi A, Richarme G.** 1999. Thermoprotection by glycine betaine and choline. Microbiology **145**:2543–2548.
50. **Chattopadhyay MK, Kern R, Mistou MY, Dandekar AM, Uratsu SL,**

Richarme G. 2004. The chemical chaperone proline relieves the thermosensitivity of a dnaK deletion mutant at 42 degrees C. J. Bacteriol. **186**: 8149–8152.
51. **Diamant S, Eliahu N, Rosenthal D, Goloubinoff P.** 2001. Chemical chaperones regulate molecular chaperones in vitro and in cells under combined salt and heat stresses. J. Biol. Chem. **276**:39586–39591.
52. **Nikaido H, Takatsuka Y.** 2009. Mechanisms of RND multidrug efflux pumps. Biochim. Biophys. Acta **1794**:769–781.
53. **Payne JW, Smith MW.** 1994. Peptide transport by micro-organisms. Adv. Microb. Physiol. **36**:1–80.
54. **Hengge R.** 2011. The general stress response in Gram-negative bacteria, p 251–289. *In* Storz G, Hengge R. (ed), Bacterial stress responses. ASM Press, Wahington, DC.
55. **Berndt C, Lillig CH, Holmgren A.** 2008. Thioredoxins and glutaredoxins as facilitators of protein folding. Biochim. Biophys. Acta **1783**:641–650.
56. **Tan JT, Bardwell JC.** 2004. Key players involved in bacteial disulfide formation. Chembiochem **5**:1479–1487.
57. **Matic I, Taddei F, Radman M.** 2004. Survival versus maintenance of genetic stability: a conflict of priorities during stress. Res. Microbiol. **155**: 337–341.
58. **Imlay JA.** 2008. Cellular defenses against superoxide and hydrogen peroxide. Annu. Rev. Biochem. **77**:755–776.
59. **Zheng M, Wang X, Templeton LJ, Smulski DR, LaRossa RA, Storz G.** 2001. DNA microarray-mediated transcriptional profiling of the *Escherichia coli* response to hydrogen peroxide. J. Bacteriol. **183**:4562–4570.
60. **Cornelis P, Wei Q, Andrews SC, Vinckx T.** 2011. Iron homeostasis and management of oxidative stress response in bacteria. Metallomics **3**:540–549.
61. **Nachin L, Loiseau L, Expert D, Barras F.** 2003. SufC: an unorthodox cytoplasmic ABC/ATPase required for [Fe-S] biogenesis under oxidative stress. EMBO J. **22**:427–437.
62. **Calhoun LN, Kwon YM.** 2011. Structure, function and regulation of the DNA-binding protein Dps and its role in acid and oxidative stress resistance in *Escherichia coli*: a review. J. Appl. Microbiol. **110**:375–386.
63. **Atlung T, Ingmer H.** 1997. H-NS: a modulator of environmentally regulated gene expression. Mol. Microbiol. **24**:7–17.
64. **Sharma UK, Chatterji D.** 2010. Transcriptional switching in *Escherichia coli* during stress and starvation by modulation of sigma activity. FEMS Microbiol. Rev. **34**:646–657.
65. **Fredriksson A, Ballesteros M, Peterson CN, Personn O, Silhavy TJ, Nystrom T.** 2007. Decline in ribosomal fidelity contributes to the accumulation and stabilization of the master stress regulator sigma S upon carbon stravation. Genes Dev. **21**:862–874.
66. **Horn G, Hofweber R, Kremer W, Kalbitzer HR.** 2007. Structure and function of bacterial cold shock proteins. Cell. Mol. Life Sci. **64**:1457–1470.
67. **Segura A, Godoy P, van Dillewijn P, Hurtado A, Arroyo N, Santacruz S, Ramos JL.** 2005. Proteomic analysis reveals the participation of energy- and stress-related proteins in the response of *Pseudomonas putida* DOT-T1E to toluene. J. Bacteriol. **187**:5937–5945.
68. **Storz G, Vogel J, Wassarman KM.** 2011. Regulation by small RNAs in bacteria: expanding frontiers. Mol. Cell **43**:880–891.
69. **Vollmer W, Bertsche U.** 2008. Murein (peptidoglycan) structure, architecture and biosynthesis in *Escherichia coli*. Biochim. Biophys. Acta **1778**: 1714–1734.
70. **Typas A, Banzhaf M, Gross CA, Vollmer W.** 2012. From the regulation of peptidoglycan synthesis to bacterial growth and morphology. Nat. Rev. Microbiol. **10**:123–136.
71. **Goldberg AL.** 2003. Protein degradation and protection against misfolded or damaged proteins. Nature **426**:895–899.
72. **Lam FC, Liu R, Lu P, Shapiro AB, Renoir JM, Sharom FJ, Reiner PB.** 2001. Beta-amyloid efflux mediated by P-glycoprotein. J. Neurochem. **76**: 1121–1128.
73. **Klucken J, Shin Y, Masliah E, Hyman BT, McLean PJ.** 2004. Hsp70 reduces alpha-synuclein aggregation and toxicity. J. Biol. Chem. **279**: 25497–25502.
74. **Magrane J, Smith RC, Walsh K, Querfurth HW.** 2004. Heat shock protein 70 participates in the neuroprotective response to intracellularly expressed beta-amyloid in neurons. J. Neurosci. **24**:1700–1706.
75. **Vashist S, Cushman M, Shorter J.** 2010. Applying Hsp104 to protein-misfolding disorders. Biochem. Cell Biol. **88**:1–13.
76. **Batelli S, Albani D, Rametta R, Polito L, Prato F, Pesaresi M, Negro A, Forloni G.** 2008. DJ-1 modulates alpha-synuclein aggregation state in a cellular model of oxidative stress: relevance for Parkinson's disease and involvement of HSP70. PLoS One **3**:e1884. doi:10.1371/journal.pone.0001884.
77. **Lopez-Otin C, Bond JS.** 2008. Proteases: multifunctional enzymes in life and disease. J. Biol. Chem. **283**:30433–30437.
78. **Ono K, Ikemoto M, Kawarabayashi T, Ikeda M, Nishinakagawa T, Hosokawa M, Shoji M, Takahashi M, Nakashima M.** 2009. A chemical chaperone, sodium 4-phenylbutyric acid, attenuates the pathogenic potency in human alpha-synuclein A30P + A53T transgenic mice. Parkinsonism Relat. Disord. **15**:649–654.
79. **Xu XM, Lin H, Maple J, Bjorkblom B, Alves G, Larsen JP, Moller SG.** 2010. The *Arabidopsis* DJ-1a protein confers stress protection through cytosolic SOD activation. J. Cell Sci. **123**:1644–1651.
80. **Gan L, Johnson DA, Johnson JA.** 2010. Keap1-Nrf2 activation in the presence and absence of DJ-1. Eur. J. Neurosci. **31**:967–977.
81. **Hayashi T, Ishimori C, Takahashi-Niki K, Taira T, Kim YC, Maita H, Maita C, Ariga H, Iguchi-Ariga SM.** 2009. DJ-1 binds to mitochondrial complex I and maintains its activity. Biochem. Biophys. Res. Commun. **390**:667–672.
82. **Gille G, Reichmann H.** 2011. Iron-dependent functions of mitochondria—relation to neurodegeneration. J. Neural Transm. **118**:349–359.
83. **O'Reilly EK, Kreuzer KN.** 2004. Isolation of SOS constitutive mutants of *Escherichia coli*. J. Bacteriol. **186**:7149–7160.
84. **Weisemann JM, Weinstock GM.** 1988. Mutations at the cysteine codons of the *recA* gene of *Escherichia coli*. DNA **7**:389–398.
85. **Adnan M, Morton G, Singh J, Hadi S.** 2010. Contribution of *rpoS* and *bolA* genes in biofilm formation in *Escherichia coli* K-12 MG1655. Mol. Cell. Biochem. **342**:207–213.
86. **Fukae J, Mizuno Y, Hattori N.** 2007. Mitochondrial dysfunction in Parkinson's disease. Mitochondrion **7**:58–62.
87. **Rothfuss O, Fischer H, Hasegawa T, Maisel M, Leitner P, Miesel F, Sharma M, Bornemann A, Berg D, Gasser T, Patenge N.** 2009. Parkin protects mitochondrial genome integrity and supports mitochondrial DNA repair. Hum. Mol. Genet. **18**:3832–3850.